



LAWRENCE  
LIVERMORE  
NATIONAL  
LABORATORY

# Characterization of the ITER CS conductor and projection to the ITER CS performance.

N. Martovetsky

June 7, 2016

29th Symposium on Fusion Technology  
Prague, Czech Republic  
September 5, 2016 through September 9, 2016

## **Disclaimer**

---

This document was prepared as an account of work sponsored by an agency of the United States government. Neither the United States government nor Lawrence Livermore National Security, LLC, nor any of their employees makes any warranty, expressed or implied, or assumes any legal liability or responsibility for the accuracy, completeness, or usefulness of any information, apparatus, product, or process disclosed, or represents that its use would not infringe privately owned rights. Reference herein to any specific commercial product, process, or service by trade name, trademark, manufacturer, or otherwise does not necessarily constitute or imply its endorsement, recommendation, or favoring by the United States government or Lawrence Livermore National Security, LLC. The views and opinions of authors expressed herein do not necessarily state or reflect those of the United States government or Lawrence Livermore National Security, LLC, and shall not be used for advertising or product endorsement purposes.

# Characterization of the ITER CS conductor and projection to the ITER CS performance

N. Martovetsky<sup>a</sup>, T. Isono<sup>b</sup>, D. Bessette<sup>c</sup>, A. Devred<sup>c</sup>, Y. Nabara<sup>b</sup>, R. Zanino<sup>d</sup>, L. Savoldi<sup>d</sup>, R. Bonifetto<sup>d</sup>, P. Bruzzone<sup>e</sup>, M. Breschi<sup>f</sup>, and L. Zani<sup>g</sup>

<sup>a</sup>US ITER Project Office, 1055 Commerce Park Dr., Oak Ridge, TN 37831, USA and  
Lawrence Livermore National Laboratory, Livermore, CA 94550, USA

<sup>b</sup>National Institutes for Quantum and Radiological Science and Technology, 801-1 Mukoyama, Naka-shi, Ibaraki-ken 311-0193 JAPAN

<sup>c</sup>ITER Organization, Route de Vinon sur Verdon, 13115 St Paul lez Durance, France

<sup>d</sup>Politecnico di Torino corso Duca degli Abruzzi 24, 10129 Torino ITALY

<sup>e</sup>Swiss Plasma Center CH 5232 - Villigen PSI Switzerland

<sup>f</sup>University of Bologna Viale Risorgimento 2, 40136, Bologna, Italy

<sup>g</sup>CEA Cadarache, 13108 St Paul lez Durance Cedex, France

The ITER Central Solenoid (CS) is one of the critical elements of the machine. The CS conductor went through an intense optimization and qualification program, which included characterization of the strands, a conductor straight short sample testing in the SULTAN facility at the [Swiss Plasma Center \(SPC\)](#), Villigen, Switzerland, and a single-layer CS Insert coil recently tested in the Central Solenoid Model Coil (CSMC) facility in Naka, Japan. We obtained valuable data in a wide range of the parameters (current, magnetic field, temperature, and strain), which allowed a credible characterization of the CS conductor in different conditions. Using this characterization, we will make a projection to the performance of the CS in the ITER reference scenario.

Keywords: Superconducting magnets, voltage measurement, strain measurement, degradation, performance

## 1. Introduction

A Central Solenoid Insert (CSI) was tested in 2015 [1] in the background field of the Central Solenoid Model Coil (CSMC).

The CSI design, analysis and fabrication are given in [2,3]. The test showed that the CSI had no degradation as a result of the cyclic electromagnetic (EM) loading or cooldown-warm up cycles. The CSI showed losses in line with expectations from the tests at SULTAN or at University of Twente, including significant reduction as a result of cycling.

One of the main goals of the CSI tests was to characterize the conductor behavior in order to compare its performance with SULTAN measurements and also and most importantly, create a predictive model for ITER CS performance.

## 2. Analysis approach

In order to characterize the CS conductor we will use a strand correlation of the critical current versus strain, magnetic field and temperature  $I_c(e, B, T)$  measured at University of Twente.

The formula for the correlation is described in [4] and parameters of the correlation for the CSI conductor are given in Table 1.

We are trying to describe performance of the conductor using a simplified model. It is well known that the strain in the 900 strand conductor has a very complex spatial distribution [5]. Also, strain comes from different sources. The superconductor is born during heat treatment at 650 C and during the cooldown to room temperature and then to the supercritical helium temperature of about 4.5 K it produces a cooldown strain, which is usually compressive and is near -0.5-0.7% for CICC in a steel jacket.

**Table 1.** Correlation of the CSI strand

Parameter	Value
Ca1	45.74
Ca2	4.431
e0a	0.00232
em	-0.00061
Bc20m	29.39
Tc0m	16.48
C1	21851
p	0.556
q	1.698

When the coil is energized, the electromagnetic (EM) force produces a hoop tensile strain and a lateral

compressive force that crushes the cable against the wall of the jacket. Both strains are proportional to the product of  $I \times B$ .

In order to find  $T_{cs}$  and the effective strain we used integrated electrical field over the cable cross section taking into account the real transition to normal state. That is done in order to take into account varying magnetic field in the cross section. The temperature and strain distribution are assumed uniform.

Usually the hoop strain improves performance and increases  $T_{cs}$ , while lateral crushing force reduces the  $T_{cs}$  due to high sensitivity of the Nb3Sn to the lateral compressive stress and bending of the strands. We, however, are trying to describe the strain in the cable with one number – “effective total strain”, which will have these three components of the strain – cooldown, longitudinal (hoop) and lateral crushing:

$$\mathcal{E}_{total} = \mathcal{E}_{cd} + \mathcal{E}_{hoop} + \mathcal{E}_{crush} \quad (1)$$

The hoop and crushing stress are both proportional to  $I \times B$ . We make an assumption that a simple addition adequately reflects the effect of these components on describing performance of the CS conductor.

We could not directly measure the cooldown strain, but we can deduce this strain extrapolating total strain to the zero EM force.

We cannot directly measure strain in the cable for obvious reasons. However, we did measure strain in the jacket. We know from the past experience that strain in the jacket is not necessarily equal to strain in the cable. However, we expect that the strain in the cable will be relatively close to and proportional to the jacket strain. We will calculate the cable strain by fitting the measured  $T_{cs}$  and then we will find a correlation with measured jacket strain.

We equipped the CSI with several strain gauges in order to measure the hoop strain in the CS conductor jacket.

We will use CSI data along with the data from SULTAN on the conductor that went into the CSI to compare the crushing strain in two conductors.

Knowing the strain in the jacket, and by constructing a correlation between the hoop strain in the jacket and the current sharing temperature of the CS conductor we should be able to predict the temperature margin in the ITER CS, which has approximately the same crushing force as in the CSI but a significantly higher hoop strain in the conductor.

### 3. CSI instrumentation

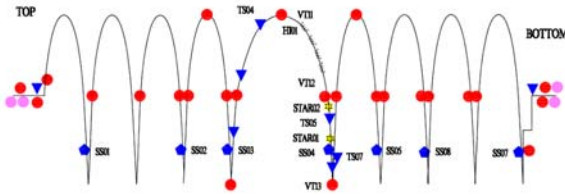


Fig. 1. Instrumentation in the CSI. Circles – temperature sensors, triangles- temperature sensors, pentagons – strain gauges.

The ability to instrument the CSI gave a unique opportunity to obtain conductor data that were not available otherwise. The CSI instrumentation schematic is shown in Fig. 1. We had seven strain gauges bonded to the conductor jacket to monitor strain in the jacket.

We measured the electrical field in the conductor using voltage taps, and we measured the temperature in the conductor. We also calculated the magnetic field distribution. All this information allowed us to build a correlation of the “effective strain” in the CS conductor, using strand correlation  $I_c(e, B, T)$  that was measured by University of Twente group.

### 4. Strain measurements in CSI

We had strain measurements on all the runs during the CSI campaign. The measurements in the beginning of the campaign were not reliable due to the signal conditioners malfunctioning. After replacing the conditioners that took place after the first warmup-cooldown cycle, the data became very stable.

The most instrumented area in the middle of the coil that develops the voltage first is represented by the strain gauge SS04. Fig. 1 shows the runs in the CSI during the test campaign that embrace CSI currents from -50 kA to 60 kA and the peak field in the CSI up to 13 T. Thus, the hoop strain changed the sign from compressive in the “reverse” charging mode to the usual tensile strain, when the field generated by CSMC and CSI coincided.

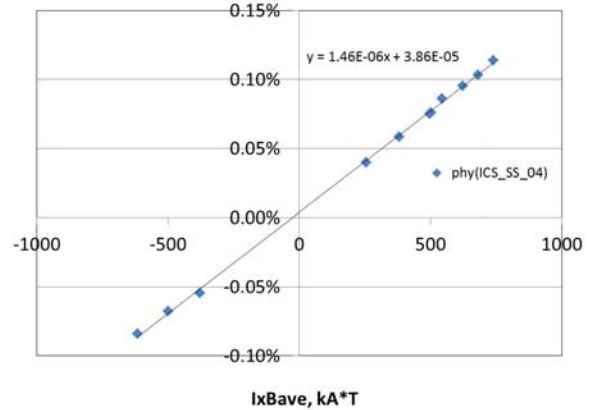


Fig. 2. Hoop strain in the CSI jacket versus electromagnetic force  $I \times B_{average}$

As can be seen, the strain is remarkably linear with the electromagnetic force, as expected, and crosses the strain line very close to zero. That completes characterization of the jacket strain versus  $I \times B$  parameter.

If the turns would support the hoop forces only by tension in the jacket, the hoop strain could be expressed as:

$$\mathcal{E}_h = \frac{IBR}{ES} \quad (2)$$

where  $I$  is the transport current,  $B$  is the average field in the cable cross section,  $R$  is the mean radius of the turn,  $S$  is the jacket cross section and  $E$  is the Young modulus of the jacket. In our case the CSI turns are spread with G-10 spacers in between [6], which carry a significant

load, so the strain in the jacket is lower. Comparing the strain from (2) with the ones that we measured, we found that only 62% of the strain calculated from (2) was measured in the jacket. This is in agreement with the ANSYS model [1].

### 5. Strain assessment in SULTAN tests

The strain in the SULTAN sample CSJA6, that has the same conductor as the CSI, can be deduced from the Tcs measurements, shown in Fig. 3.

SULTAN tests have only cooldown strain and the crushing strain, no hoop strain. During testing the Tcs is improved until saturation after 10000 cycles and therefore we process only the data after stabilization. In the CSI the improvement of the Tcs is much less pronounced but again, we process the Tcs obtained towards the end of the campaign.

Effective strain versus IxB crushing force in SULTAN is shown in Fig. 4.

The Tcs data, which were used for assessment of strain, are given in Table 2 [7].

**Table 2.** Tcs results from SULTAN tests of the CSJA6 (Right leg)

B, T	I, kA	T <sub>cs</sub> , K
10.85	45.1	7.20
10.85	40	7.46
10.4	40	7.77
9.95	40	8.11
10.85	30	7.99
10.4	30	8.295

It correlates reasonably well with the lateral crushing force IxB and extension of the trend to the zero IxB parameter suggests the effective cooldown strain of -0.61% and the crushing strain coefficient is:

$$\varepsilon_{crush} = 1.27 \cdot 10^{-6} \cdot IxB[kAT] \quad (3)$$

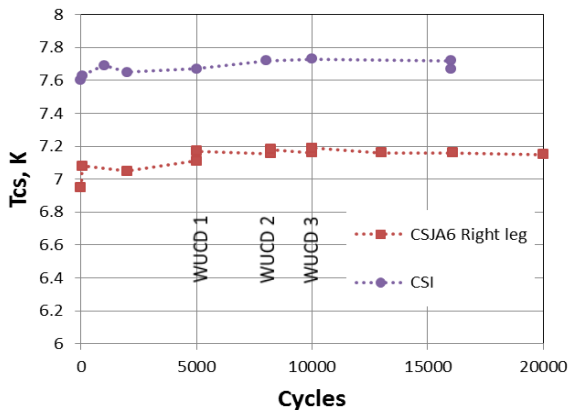


Fig. 3. Tcs evolution in CSI and SULTAN CSJA6 at comparable conditions

### 6. Strain assessment in the CSI

Fig. 5 shows assessment of the effective strain in the CSI in both modes of operation – direct charge, when the CSI and CSMC field directions coincide and in the

reverse charge mode, when the currents are opposite and CSI is compressed in hoop direction by the CSMC magnetic field. Although the vector of force changes its direction we speculate that behavior of the CSI conductor does not depend on the crushing force direction, only on the value. The Tcs performance, however, is very sensitive to the direction of the hoop strain.

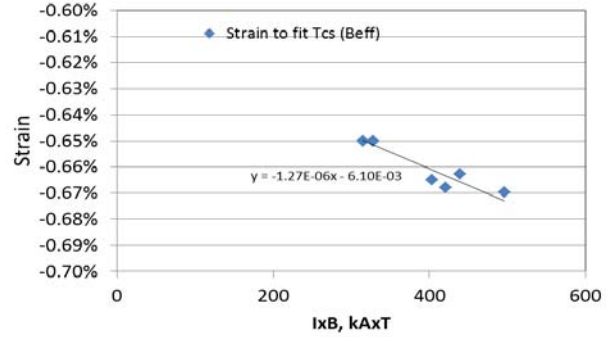


Fig.4. Effective strain in the CSJA6 SULTAN tests

The strain shown in Fig. 5 gives some interesting observations. Extension of the strain to the zero IxB from the direct charge suggests cooldown strain to be negative -0.59%. Extension of the strain line to zero IxB from the reverse charge data points at -0.58%, which is a good agreement, although a little lower than -0.61% that was observed in SULTAN measurements.

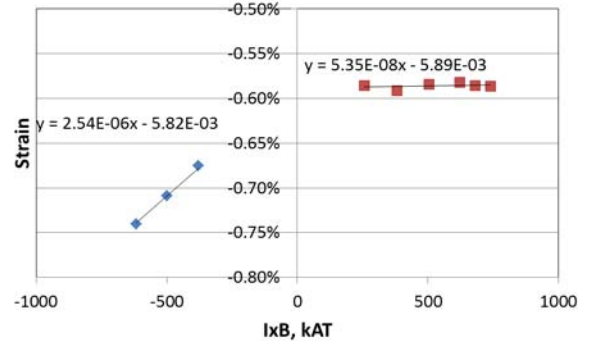


Fig. 5. Effective strain in CSI deduced from Tcs measurements

The remarkable part is that in direct charge, the hoop strain in the cable and the crushing strain balance each other almost ideally. In the reverse charge part the crushing strain and the hoop strain combine to reduce Tcs, which gives the following dependence versus IxB in CSI:

$$\begin{aligned} \varepsilon_{cd} &= -0.585\% \\ \varepsilon_{hoopcable} &= 1.27 \cdot 10^{-6} IB = \alpha \varepsilon_{hoopjacket} \\ \varepsilon_{crush} &= -1.27 \cdot 10^{-6} IB \end{aligned} \quad (4)$$

where the current I is expressed in [kA] and B is expressed in [T],  $\alpha$  is the correlation coefficient between strain in the cable and strain in the jacket.

It is desirable to express the hoop strain in the cable as a function of strain in the jacket, since our dependence of the hoop strain versus parameter IxB is only good for

the CSI, while the crushing strain is supposed to be a universal for the conductor.

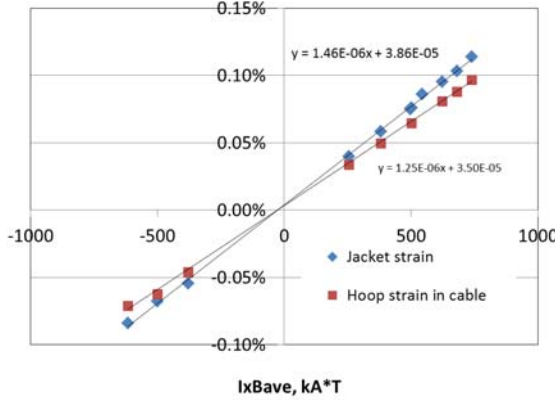


Fig. 6. Hoop strain in the jacket vs hoop strain in the cable in CSI tests.

Fig. 6 shows comparison of the measured hoop strain in the jacket versus deduced hoop strain in the cable. As we can see, the hoop strain in the cable represents about 85% of the jacket, thus we can express the correlation between the hoop strain in the cable and in the jacket as:

$$\varepsilon_{hoopcable} = 0.85\varepsilon_{hoopjacket} \quad (5)$$

It is interesting to compare the crushing force dependence vs IxB in SULTAN and CSI. Fig. 7 gives such a comparison, which shows a very similar pattern.

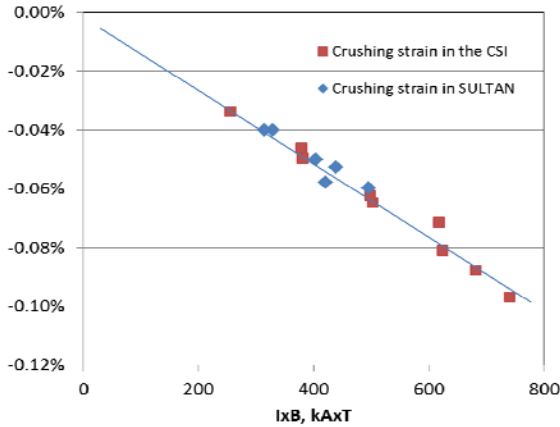


Fig. 7. Crushing strain in CSI and SULTAN

## 7. Projection of CS conductor behavior in the ITER CS

With the established correlations of the crushing and hoop strains we now can project the current sharing temperature in the ITER CS in the most stringent condition, which is the Initial Magnetization, right before the plasma initiation.

Let's make a prediction for the Tcs in the ITER CS at IM. Peak average longitudinal strain in the CS jacket in the CS at IM (0.19%), effective field (B = 12.6 T) and a current (40 kA) are known, the effective strain in the cable will be:

$$\begin{aligned} \varepsilon_{total} &= -0.59\% + 0.19\% * 0.85 \\ &- 1.27 * 10^{-6} * 40 * 12.6 = -0.49\% \end{aligned} \quad (6)$$

Thus, effective strain in the CS will be improved by 0.1% in comparison with CSI. That reduction in the compressive strain should give about 0.6 K additional temperature margin at IM to Tcs=7.35 K in comparison with the CSI data at IM conditions because the hoop strain in the CS is significantly higher than in the CSI, while the crushing force is the same.

The original acceptance criterion for CS Tcs at IM is 5.2 K.

At the end of burn conditions in ITER operation, the hoop EM strain in the ITER CS jacket will be 0.176% in comparison with the CSI, where we measured 0.086%. This increase of the hoop strain will result in increase of the Tcs parameter by 0.6 K from 6.97 K measured in the CSI to 7.57 K. This is a very significant increase in temperature margin of the CS magnet that improves reliability and robustness of the machine.

## 8. Conclusions

The SULTAN and CSI test data demonstrated again sensitivity of the large CICC with Nb3Sn strands to the strains. Using test data and a simplified model we characterized the conductor behavior in terms of three components of the strain – cooldown, longitudinal and lateral crushing strains. We see that effect of the crushing force on the performance of the conductor is similar in the straight sample in SULTAN tests and in a solenoid of CSI. The hoop strain effect predicts that ITER CS will have an additional significant margin, which gives an additional assurance in CS successful operation.

## 9. Acknowledgements

This manuscript has been authored by UT-Battelle, LLC under U.S. Department of Energy Contract No. DE-AC05-00OR22725 and LLNL under DOE Contract No. DE-AC52-07NA27344. The United States Government retains and the publisher, by accepting the article for publication, acknowledges that the United States Government retains a non-exclusive, paid-up, irrevocable, world-wide license to publish or reproduce the published form of this manuscript, or allow others to do so, for United States Government purposes.

*The views and opinions expressed herein do not necessarily reflect those of the ITER Organization.*

## References

- [1] N. Martovetsky, T. Isono, D. Bessette et al, "ITER Central Solenoid Insert Test Results", *IEEE Trans. Appl. Supercond.*, to be published in 2016
- [2] Y. Nabara, T. Hemmi, H. Kajitani et al, "Impact of Cable Twist Pitch on Tcs-Degradation and AC Loss in Nb3Sn Conductors for ITER Central Solenoids" *IEEE Trans. Applied Supercond.* vol. 24, no. 3, June 2014 p. 4200705
- [3] A. E. Khodak, N. N. Martovetsky, A. V. Smirnov, P. H. Titus, "Optimization of ITER Central Solenoid Insert design", *Fusion Engineering and Design, Volume 88*, Issues 9–10, Oct 2013, pp 1523-1527
- [4] Luca Bottura and Bernardo Bordini, "Jc(B,T,Σ) parameterization of the ITER Nb3Sn production," *IEEE*

- Trans. Appl. Supercond.*, vol. 19, no. 3, 2009, pp.1521–1524.
- [5] H. Bajas, D. Durville, D. Ciazynski, and A. Devred, “Numerical Simulation of the Mechanical Behavior of ITER Cable-In-Conduit Conductors”, *IEEE Trans. Appl. Supercond.*, vol. 20, no. 3, 2010, pp.1467–1470
  - [6] T. Isono, K. Kawano, H. Ozeki et al., “Fabrication of an Insert to Measure Performance of ITER CS Conductor”, *IEEE Trans. Applied Supercond.* vol. 25, no. 3, June 2015 p. 4201004
  - [7] CSJA6 SULTAN Sample Test Report, CRPP report June 2014